

Statistical properties of continuous-wave Bloch oscillations in double-well semiconductor heterostructures

A. N. Korotkov, D. V. Averin, and K. K. Likharev

*Department of Physics, State University of New York, Stony Brook, New York 11794-3800
and Department of Physics, Moscow State University, Moscow 119899 GSP, Russia*

(Received 1 October 1993)

Starting from a simple model of the double-well semiconductor heterostructure capable of generating continuous-wave quantum "Bloch" oscillations, we have calculated analytically their major statistical properties, including spectral density and amplitude distribution. Other characteristics of the structure, pertaining to the Bloch oscillation, such as the dc I - V curve, rf impedance, and dc response to an external rf signal, were also calculated. The results are used to discuss similarities and differences between the Bloch oscillations and other types of oscillatory processes including the Josephson oscillations, laser radiation, spontaneous radiation, and narrow-band random noise.

I. INTRODUCTION

Recently there has been a revival of interest in quantum "Bloch" (or "Stark," or "Rabi") oscillations which can be induced in solid state structures biased by dc electric field E . The frequency of these oscillations is given by the fundamental quantum relation $\omega = \Delta W/\hbar$, where ΔW is the change of the electron energy due to its transition from one state to another; in the simplest case of a periodic structure $\Delta W = eEd$, where d is the spatial period. Although the Bloch oscillations have been discussed theoretically for a long time now,¹⁻³ especially after the advent of the semiconductor heterostructures^{4,5} (see also reviews⁶⁻⁸) until very recently the experimental situation was much less encouraging. Observation of continuous-wave Bloch oscillations in the main candidate structures, long semiconductor superlattices,⁴⁻⁶ is considerably hindered by the effects of electric charge accumulation.^{9,10} These effects are less forbidding for short pulses of Bloch oscillations which can be induced by short light pulses pumping a small number of electrons into an initially empty well or miniband of a heterostructure.¹² Such pulses have been observed recently from double-well^{13,14} and multiwell¹⁵ heterostructures. (Note that the Bloch dynamics of these two systems is similar in the most interesting high-field limit.)

These remarkable experiments invite further theoretical studies of the Bloch oscillators as possible radiation sources in the submillimeter wave band, including not only their power and frequency, but also statistical properties such as spectral density distribution (in particular, linewidth) and amplitude statistics. Such calculations, to the best of our knowledge, have never been carried out for Bloch oscillations, with the single exception of a Monte Carlo calculation of the spectral density of electron velocity in lateral superlattices for one particular set of parameters.¹⁶ This is why obtaining analytical expressions for the statistical characteristics was the main goal of this work.

We have concentrated on the continuous-wave oscil-

lation mode as the most interesting one. A double-well (rather than a multiwell) structure,¹⁷ was selected for our analysis because that is the most straightforward way to circumvent the charge accumulation instabilities typical for this mode.

The paper is organized as follows. In Sec. II we introduce a relatively simple model of the double-well heterostructure and derive its basic equations. In Sec. III we calculate the dc I - V characteristic of the structure and compare our results with those obtained earlier by other authors. Section IV is devoted to statistical properties of the Bloch oscillations, determined by the multielectron nature of the oscillations. We have found it enlightening to contrast the results for "autonomous" oscillations (induced by dc electric field) with their characteristics under the influence of a weak external rf radiation with a frequency close to the Bloch oscillation frequency. Calculations of these characteristics are described in Sec. V. One of the results, the rf conductance of the system, has allowed us to find the available power of Bloch oscillations (Sec. VI). In conclusion (Sec. VII), we use the results obtained in the preceding sections to discuss the position of the Bloch oscillations in the row of other self-oscillatory physical phenomena, including Josephson oscillations, laser radiation, and spontaneous radiation.

II. MODEL AND BASIC EQUATIONS

We will consider processes in the semiconductor double-well structure with the band-edge diagram shown in Fig. 1. Quantization of the electron motion along the z axis (perpendicular to the layers) leads to formation of subbands in quantum wells 1 and 2, so that the electron energy in the i th well ($i = 1, 2$) in the lowest subband can be presented as

$$\varepsilon_i(p) = \varepsilon_i(0) + p^2/2m, \quad (1)$$

where $\mathbf{p} \perp \mathbf{n}_z$ is the transverse momentum. We chose the zero of energy in such a way that the bottom values $\varepsilon_1(0)$

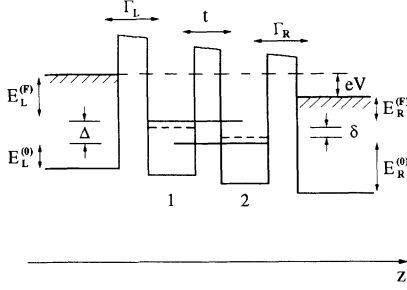


FIG. 1. Edge-band diagram of the double-well heterostructure considered in this work. Energy levels of electrons with zero transverse momentum p are shown by solid lines, while dashed lines show these levels in the absence of the coupling between the wells ($t = 0$). In this work, we consider the case $\hbar\Gamma_{L,R}, \hbar\Gamma \ll \Delta \ll E_{L,R}^{(0)}, E_{L,R}^{(F)}$, though our main qualitative conclusions are hardly dependent on this assumption.

and $\varepsilon_2(0)$, which are shown by dashed lines in Fig. 1, can be written as

$$\varepsilon_1(0) = \delta/2, \quad \varepsilon_2(0) = -\delta/2.$$

The parameter δ reflects both a possible initial asymmetry of the wells and the effect of the dc voltage V between external electrodes, a part ηV of which drops between the wells:

$$\delta = \delta_0 + \eta eV. \quad (2)$$

The factor $\eta < 1$ is determined by the ratio of capacitances between the wells and external electrodes; typically η is close to $1/3$.

As usual, we will assume that electrons can tunnel through the barriers separating the wells without changing their transverse momentum p . Then the Hamiltonian of the structure can be presented as follows:

$$H = H_0 + H_L + H_R + H_{\text{scatt}}, \quad (3)$$

where

$$H_0 = \sum_p [\varepsilon_1(p) a_p^\dagger a_p + \varepsilon_2(p) b_p^\dagger b_p - \frac{t}{2} (a_p^\dagger b_p + \text{H.c.})], \quad (4)$$

$$H_L = \sum_q \varepsilon_L(q) c_q^\dagger c_q + t_{Lq} (c_q^\dagger a_p + \text{H.c.}), \quad (5)$$

and H_R is given by a similar expression with $L \rightarrow R$. Here $a, a^\dagger, b, b^\dagger, c, c^\dagger$ are the corresponding creation and annihilation operators, and q is the momentum of electron motion in the external electrode. (In the following calculations we will assume that the area of the structure is not too small and hence the spectra $\varepsilon_{L,R}(q)$ and $\varepsilon_{1,2}(p)$ are continuous on the energy scale of interest.)

The Hamiltonian

$$H_{\text{scatt}} = \sum_{p,p'} [V_1(p,p') a_p^\dagger a_{p'} + V_2(p,p') b_p^\dagger b_{p'}] \quad (6)$$

describes elastic scattering of the electrons inside the quantum wells. Our main assumption will be that the

scattering rate Γ , as well as the rates of tunneling through the edge barriers $\Gamma_{L,R}$, is small in comparison with the net splitting of the energy levels due to tunneling between the wells

$$\Delta = (\delta^2 + t^2)^{1/2}. \quad (7)$$

In this case it is convenient to diagonalize H_0 (for each p):

$$H_0 = \sum_p [\varepsilon_+(p) \alpha_p^\dagger \alpha_p + \varepsilon_-(p) \beta_p^\dagger \beta_p], \quad (8)$$

where

$$\alpha_p^\dagger = a_p^\dagger \cos \phi - b_p^\dagger \sin \phi, \quad \beta_p^\dagger = b_p^\dagger \cos \phi + a_p^\dagger \sin \phi, \\ \phi = \arctan[(\Delta - \delta)/t], \quad 0 < \phi < \pi/2, \quad (9)$$

and

$$\varepsilon_\pm(p) = \frac{p^2}{2m} \pm \frac{\Delta}{2}. \quad (10)$$

It is straightforward to express H_L, H_R , and H_{scatt} in this new basis and, treating these terms as perturbations, find dynamics of the single-particle density matrix elements

$$\rho_{pp'}^{\alpha\alpha} = \langle \alpha_p^\dagger \alpha_{p'} \rangle, \quad \rho_{pp'}^{\beta\beta} = \langle \beta_p^\dagger \beta_{p'} \rangle, \\ \rho_{pp'}^{\alpha\beta} = (\rho_{p'p}^{\beta\alpha})^* = \langle \alpha_p^\dagger \beta_{p'} \rangle, \quad (11)$$

where $\langle \dots \rangle$ denotes averaging over the true multiparticle density matrix.¹⁹ In the usual Markov approximation these equations are reduced to equations for diagonal (in p) elements

$$n_1(p) \equiv \rho_{pp}^{\alpha\alpha}, \quad n_2(p) \equiv \rho_{pp}^{\beta\beta}, \quad r(p) \equiv \rho_{pp}^{\alpha\beta}, \quad (12)$$

which, in our approximation (1), do not depend on the direction of \mathbf{p} :

$$\dot{n}_1(p) = \Gamma_L \cos^2 \phi [f_L(\varepsilon_+(p)) - n_1(p)] \\ + \Gamma_R \sin^2 \phi [f_R(\varepsilon_+(p)) - n_1(p)] \\ + \Gamma \sin^2 \phi \cos^2 \phi [n_2(p_+) - n_1(p)], \quad (13)$$

$$\dot{n}_2(p) = \Gamma_L \sin^2 \phi [f_L(\varepsilon_-(p)) - n_2(p)] \\ + \Gamma_R \cos^2 \phi [f_R(\varepsilon_-(p)) - n_2(p)] \\ + \Gamma \sin^2 \phi \cos^2 \phi [n_1(p_-) - n_2(p)],$$

$$\dot{r}(p) = (-i\Delta/\hbar - \gamma) r_p, \quad \gamma \equiv \frac{1}{2} (\Gamma_L + \Gamma_R + \Gamma). \quad (14)$$

In these equations p_\pm are defined by the relations $p_\pm^2/2m = p^2/2m \pm \Delta$, and

$$\Gamma_{L,R} \equiv \frac{2\pi}{\hbar} |t_{L,R}|^2 \rho_{L,R}$$

$$\Gamma \equiv \frac{2\pi}{\hbar} |V_1(pp') - V_2(pp')|^2 \rho,$$

where $\rho_{L,R}$ are the densities of states in the external electrodes, while $\rho = Sm/\pi\hbar^2$ is the two-dimensional (2D) density of states in the wells (S is the structure area). In what follows, we will assume that the rates Γ and $\Gamma_{L,R}$

do not depend on energy, and hence on p . This assumption requires, in particular, the quantization levels to be well above the conduction band edge in the external electrodes (Fig. 1): $E_L^{(0)}, E_R^{(0)} \gg \Delta$.

Note that the master equations (13) have a clear physical meaning, describing a detailed balance of electrons with momentum p on their two effective energy levels $\varepsilon_{\pm}(p)$, while the equation (14) for the off-diagonal matrix element describes the decay of the quantum coherence between electrons on these levels. Generally, the system of Eqs. (13), (14) is typical for homogeneously broadened two-level quantum systems (see, e.g., Ref. 20). Probably the only feature specific to semiconductor heterostructures is that generally there are many two-level systems, each with a specific value of the transverse momentum p , but with the same level splitting Δ , and all these systems are coupled via scattering [described in Eqs. (13) by the terms proportional to Γ]. For practical calculations, it is easier to make a change of variables, $p_- \rightarrow p$, $p \rightarrow p_+$, in the equation for n_2 . The resulting equations for $n_1(p)$ and $n_2(p_+)$ form a closed system, so that the summation over p (necessary for calculation of the observable variables) can be carried out at the final stage, after solution of this system.

III. dc $I - V$ CHARACTERISTIC

It is evident from Eqs. (13) that the dc current \bar{I} flowing through the system can be expressed as follows:

$$\begin{aligned} \bar{I} &= e\Gamma_L \sum_p (\cos^2 \phi [f_L(\varepsilon_+(p)) - n_1(p)] \\ &\quad + \sin^2 \phi [f_L(\varepsilon_-(p)) - n_2(p)]) \\ &= -e\Gamma_R \sum_p (\sin^2 \phi [f_R(\varepsilon_+(p)) - n_1(p)] \\ &\quad + \cos^2 \phi [f_R(\varepsilon_-(p)) - n_2(p)]), \end{aligned} \quad (15)$$

via stationary solution $n_{1,2}(p)$ of these equations. The resulting formula is quite simple for the most interesting case when the quantization levels $\pm\Delta/2$ are located well below the Fermi levels in both external electrodes (Fig. 1):

$$E_{L,R}^{(F)} \gg T, \quad (16)$$

where T is the temperature in energy units. In this limit the current can be expressed as

$$\bar{I} = 2e^2 \rho V \gamma \left(\frac{(\Gamma_L \cos^2 \phi + \Gamma_R \sin^2 \phi)(\Gamma_L \sin^2 \phi + \Gamma_R \cos^2 \phi)}{\Gamma_L \Gamma_R \sin^2 \phi \cos^2 \phi} + \Gamma \frac{\Gamma_L + \Gamma_R}{\Gamma_L \Gamma_R} \right)^{-1}. \quad (17)$$

Figure 2(a) shows the dependence of the \bar{I}/V ratio on the asymmetry parameter δ . One can see that this ratio peaks at $\delta = 0$, when the energy levels in the wells are aligned. The width of this peak, in terms of δ , is of the order of

$$\Delta\delta = t \left(\frac{\gamma(\Gamma_L + \Gamma_R)}{\Gamma_L \Gamma_R} \right)^{1/2} > t. \quad (18)$$

This resonance dependence shows up in the dc $I - V$ characteristics of the structure [Figs. 2(b) and 2(c)], because the applied voltage V changes δ [see Eq. (2)]. If the structure was initially asymmetrical ($|\delta_0| \gg t$), the peak in the $I - V$ characteristic [Fig. 2(b)] is very similar to that shown in Fig. 2(a). In the initially symmetrical structure ($|\delta_0| \ll t$) [see Fig. 2(c)], the resonance peak is, however, distorted from its "seed" shape shown in Fig. 2(a) since it is very close to the origin, where the current is suppressed by the smallness of the number of available states in the external electrodes [this effect is described by the factor V in Eq. (17)]. Note that the width of the dc current peak (in energy units) always exceeds the tunneling amplitude t , i.e., with our assumptions, the peak is much wider than Γ and $\Gamma_{L,R}$.

In the limit $\Gamma \ll \Gamma_{L,R}$ our expression coincides with that obtained by Gurvitz,²¹ who solved a similar problem for a system without scattering. More generally, the negative-slope regions of the dc $I - V$ curves, similar to those shown in Fig. 2, are typical for virtually all structures capable of generating the Bloch oscillations⁴⁻¹¹ and other systems with resonance tunneling.

IV. BLOCH OSCILLATION STATISTICS

In accordance with Eq. (4), the operator of the current $I(t)$ flowing between the quantum wells can be presented as

$$I(t) = ie \frac{t}{2\hbar} \sum_p (a_p^\dagger b_p - b_p^\dagger a_p) = ie \frac{t}{2\hbar} \sum_p (\alpha_p^\dagger \beta_p - \beta_p^\dagger \alpha_p). \quad (19)$$

In order to calculate the spectral density

$$S_I(\omega) = 4 \int_0^\infty K(\tau) \cos \omega \tau d\tau \quad (20)$$

of the current, we should find its symmetrized correlation function

$$K(\tau) = \frac{1}{2} \langle I(t)I(t+\tau) + I(t+\tau)I(t) \rangle. \quad (21)$$

[Our choice of the numerical factor in Eq. (20) corresponds to relation $S_I(\omega) = \langle I_\omega^2 \rangle / (\Delta\omega/2\pi)$, where I_ω is the component of the current $I(t)$ within a narrow interval $\Delta\omega$ around an observation frequency ω .]

A straightforward calculation using Eqs. (13), (14), and (19)–(21) yields

$$S_I(\omega) = \frac{e^2 t^2}{2\hbar^2} \frac{\gamma}{(\omega - \omega_B)^2 + \gamma^2} \Sigma, \quad (22)$$

$$\Sigma = \sum_p \langle \alpha_p^\dagger \alpha_p \beta_p \beta_p^\dagger + \alpha_p \alpha_p^\dagger \beta_p^\dagger \beta_p \rangle, \quad \omega > 0,$$

where $\omega_B \equiv \Delta/\hbar$. According to Eq. (14), in the station-

ary regime $r_p = 0$, i.e., there is no coherence between states on the levels $\varepsilon_\pm(p)$, so that

$$\Sigma = \sum_p \{n_1(p)[1 - n_2(p)] + n_2(p)[1 - n_1(p)]\},$$

and we can evaluate the sum using the stationary solution of Eq. (13):

$$\sum_p n_1(p)[1 - n_2(p)] = \frac{\rho}{(a+b)^2} [g(-\Delta)(ac+bd) + g(-\Delta - eV)ad + g(-\Delta + eV)bc],$$

$$\sum_p n_2(p)(1 - n_1(p)) = \frac{\rho}{(a+b)^2} [g(\Delta)(ac+bd) + g(\Delta + eV)ad + g(\Delta - eV)bc], \quad (23)$$

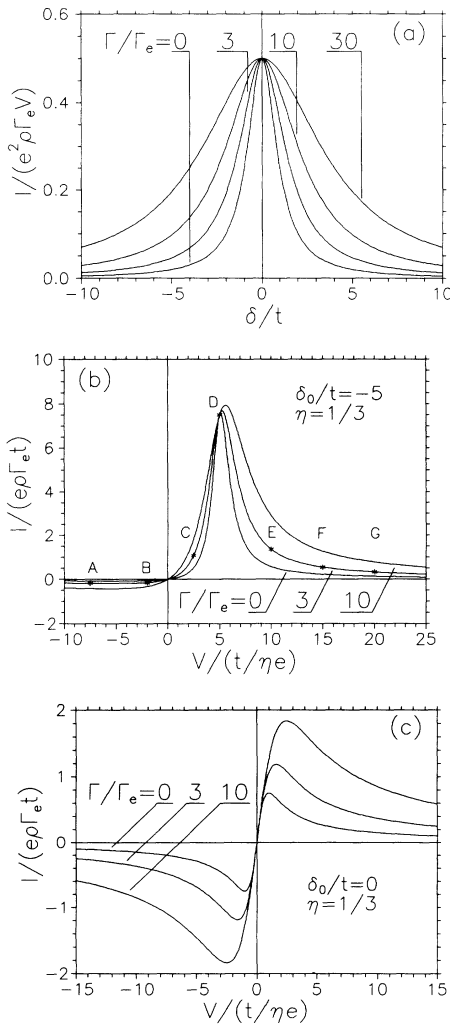


FIG. 2. dc current through the quantum double-well structure as a function of (a) the asymmetry factor δ , and (b), (c) the applied dc voltage V , for various intensities of the elastic scattering Γ at $\Gamma_L = \Gamma_R \equiv \Gamma_e$. (b) shows the results for an asymmetric structure, while (c) shows the results for the initially symmetric structure. Points in (b) indicate a set of parameters for plots in Figs. 3, 4, and 6.

where $g(x) = x/(1 - \exp(-x/T))$, and

$$a = \Gamma_L \sin^2 \phi (\Gamma_L \cos^2 \phi + \Gamma_R \sin^2 \phi + \Gamma \cos^2 \phi),$$

$$b = \Gamma_R \cos^2 \phi (\Gamma_L \cos^2 \phi + \Gamma_R \sin^2 \phi + \Gamma \sin^2 \phi),$$

$$c = \Gamma_L \cos^2 \phi (\Gamma_L \sin^2 \phi + \Gamma_R \cos^2 \phi + \Gamma \sin^2 \phi),$$

$$d = \Gamma_R \sin^2 \phi (\Gamma_L \sin^2 \phi + \Gamma_R \cos^2 \phi + \Gamma \cos^2 \phi).$$

Figure 3 shows the spectral density as a function of the observation frequency ω for several values of the dc voltage V (the corresponding bias points are marked in Fig. 2). In the particular case when the “detuning” $|\delta|$ is larger than t , so that the electron wave functions are strongly localized in the wells, the Fermi levels in the wells coincide with those of the external electrodes [these conditions are satisfied when the bias point lies outside the peak (18) of the dc current]. Then, if the temperature

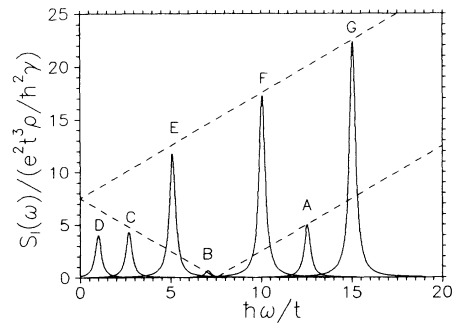


FIG. 3. Spectral density of the tunneling current $I(t)$ through an asymmetric system ($\delta_0 = -5t$) as a function of the observation frequency ω , for $\Gamma/\Gamma_e = 3$, $\hbar\gamma/t = 0.2$ and several values of the dc voltage [the corresponding dc bias points are indicated in Fig. 2(b)]. The dashed line shows the amplitude of the peak in spectral density according to Eq. (24) which is valid for dc bias voltages outside of the resonant peak in the dc $I - V$ curve.

is much smaller than $|eV - \delta|$, one has $\Sigma = \rho |eV - \delta|$, and

$$S_I(\omega) = \frac{e^2 t^2}{2\hbar^2} \frac{\gamma}{(\omega - \omega_B)^2 + \gamma^2} \rho |eV - \delta|, \quad \text{for } \omega \simeq \omega_B. \quad (24)$$

This formula shows clearly that $S_I(\omega)$ peaks at the Bloch oscillation frequency, $\omega_B = \Delta/\hbar$, and that the linewidth of the oscillations is 2γ . The height of the peak vanishes at a particular value of the dc voltage, $V = \delta_0/e(1 - \eta)$, where the factor $|eV - \delta|$ is zero, and grows proportionally to the absolute deviation from that point (where quantum wells contain the same number of electrons and the net amplitude of the Bloch oscillations vanishes).

Thus, the dc-biased double-well structure may exhibit continuous-wave narrow-band Bloch oscillations (in contrast to the conclusion reached in the recent work²¹), and the amplitude of these oscillations increases with increasing asymmetry of the structure. Note, however, that $S_I(\omega)$ does not present the available power density for two reasons.

At $\omega \neq 0$, the tunneling current between the wells is not equal to the current in the external circuit, due to the shunting effect of capacitances between the layers and currents flowing between the wells and external electrodes;

$S_I(\omega)$ as calculated above contains a zero-point contribution.

We will come back to these problems in Sec. VI.

Now let us note that according to Eqs. (13), (14), and (24), in the limit $\gamma \ll \omega_B$ the Bloch oscillations can be considered as a sum of independent oscillators of the same frequency $\omega_B = \Delta/\hbar$ with the amplitude $et/2\hbar$ and linewidth γ each. This implies that the net oscillation amplitude A_B is distributed with the probability density

$$\rho(A_B) = \frac{2A_B}{D} \exp(-A_B^2/D), \quad D = \left(\frac{et}{2\hbar}\right)^2 \Sigma. \quad (25)$$

Such a wide distribution is typical for the amplitude of the spontaneous radiation (or a white noise passed through a narrow-band filter).

V. EFFECTS OF EXTERNAL RADIATION

We can describe effects of irradiation of the double-well structure by external monochromatic signal of frequency

$$\sum_p [n_1(p) - n_2(p)] = \rho \{ eV \Gamma_L \Gamma_R (\cos^2 \phi - \sin^2 \phi) [(\Gamma_L \sin^2 \phi + \Gamma_R \cos^2 \phi) \times (\Gamma_L \cos^2 \phi + \Gamma_R \sin^2 \phi) + \Gamma \sin^2 \phi \cos^2 \phi (\Gamma_L + \Gamma_R)]^{-1} - \Delta \}. \quad (30)$$

The factor η in Eq. (28) takes into account the fact that the current $I_e(t)$ induced by the tunneling current $I(t)$ between the wells is smaller than $I(t)$,

$$I_e(t) = \eta I(t). \quad (31)$$

$\omega \sim \omega_B$ by addition of the term

$$V_{rf} = \text{Re}[V_A e^{i\omega t}] \quad (26)$$

to the dc voltage V applied to the structure. Such a description is valid when the effective external admittance $|Y_{ef}(\omega)|$ [where $Y_{ef}(\omega) = Z_e^{-1}(\omega) + i\omega C$, $Z_e(\omega)$ is the external circuit impedance, and C is the structure capacitance] is much higher than the tunneling admittance $Y_T \sim |I_T/V_A|$. For typical structures in the frequency range of interest ($\omega \sim 10^{12-14} \text{ s}^{-1}$), $Y_T \ll \omega C$, so that the above condition is fulfilled regardless of the value of $Z_e(\omega)$ and structure area S .

The rf voltage (26) results in oscillation of the detuning δ with the amplitude $\tilde{\delta} = \eta e V_A$, and generally affects the eigenfunctions of the Hamiltonian H_0 . If $\eta e V_A$ is much less than Δ , one can, however, describe the influence of V_A on the eigenfunctions of H_0 in the linear approximation, while the ratio between $\tilde{\delta}/\hbar$ and all Γ 's can still be arbitrary. In this "small-signal" approximation, Eq. (14) takes the form

$$\dot{R}_p = [i(\omega - \omega_B) - \gamma] R_p + i \frac{\tilde{\delta}}{2\hbar} \sin \phi \times \cos \phi [n_1(p) - n_2(p)], \quad R_p \equiv r_p e^{i\omega t}. \quad (27)$$

Substituting the stationary solution of this equation into Eq. (19), we find that the tunneling current $I(t)$ acquires an additional component at the signal frequency ω , with the complex amplitude

$$I_A \equiv \langle I(t) e^{-i\omega t} \rangle,$$

proportional to V_A . For their ratio

$$Y(\omega) = I_A / \eta V_A, \quad (28)$$

which is essentially the small-signal (differential) admittance of the structure due to the tunneling current, these equations yield

$$Y(\omega) = -i \frac{e^2 t}{2\hbar^2} \sin \phi \cos \phi \frac{1}{\omega - \omega_B + i\gamma} \times \sum_p [n_1(p) - n_2(p)] \quad \text{for } \omega \simeq \omega_B, \quad (29)$$

where the sum in the right-hand side can be evaluated from the unperturbed master equations (13):

The coefficient η in this equation is the same one that participated in Eq. (2). [One can prove this by noting that the elementary work of the external electric field on the small charge $dQ = Idt$ transferred between the wells can be written as either $(\eta V)dQ$ or VdQ_e , where $dQ_e = I_e dt$.]

Note also that in the definition (28) we have disregarded the effect of the external rf signal on the currents flowing between the wells and external electrodes. This is legitimate at $\omega \simeq \omega_B$, where the response to the resonant rf radiation is dominated by the tunneling current flowing between the wells, which oscillates with this frequency.

Figure 4(a) shows the rf conductance (the real part of the rf admittance) as a function of the external signal frequency for the same values of the dc voltage as in Fig. 3 [see points in Fig. 2(b)], while Fig. 4(b) shows the imaginary part of the admittance for the same bias points. One can see that the rf conductance peaks at $\omega \simeq \omega_B$ can be either positive or negative. Equation (30) says that, crudely, the conductance is positive on the left slope of the resonance peak of the dc current [see Fig. 2(b)] while it is negative on the right slope of the peak. For relatively low frequencies ($\hbar\omega \ll |\Delta|$) this change of sign is clearly understandable as a result of the change in the slope of the dc $I - V$ curve. Let us emphasize, however, that the result is valid for much higher frequencies $\omega \sim \omega_B$, where it can be more naturally interpreted as a result of stimulated photon emission by the set of two-level systems with the dc current-induced population inversion:

$$\sum_p [n_1(p) - n_2(p)] > 0.$$

This result implies that the double-well structures can be used not only for generation of (relatively broad-band) spontaneous Bloch oscillations with central frequency ω_B , but also for amplification of external signals with frequency close to ω_B . This effect can also be used for excitation of narrow-band autonomous oscillations with frequencies close to ω_B in high- Q resonant cavities with intrinsic bandwidth less than γ . Such oscillators would be very similar in their physical properties to conventional lasers, but would be suitable for the generation of coherent stimulated radiation in the terahertz frequency range (probably the abbreviation “taser” is more appropriate in this case).

The main new effect which appears in higher approximations in V_A is a contribution to the dc current \bar{I} .²² This effect can be readily calculated still assuming $\delta \ll \Delta$, but

$$\bar{I} = 2e\Gamma_L\Gamma_R\rho\gamma \frac{eV + [eV + \Delta(\sin^2\phi - \cos^2\phi)]z}{\Gamma_L\Gamma_R(\sin^{-2}\phi \cos^{-2}\phi - 4) + 2\gamma(\Gamma_L + \Gamma_R)(1+z)}, \quad z \equiv \frac{(\eta eV_A/2\hbar)^2}{(\omega - \omega_B)^2 + \gamma^2}, \quad (32)$$

is a generalization of Eq. (17).

Figure 5 shows the effect of the monochromatic radiation on dc $I - V$ characteristic of the system, for several values of the signal frequency. One can see that the weak radiation is only important within narrow intervals ($\Delta\omega \sim \gamma$) around the Bloch oscillation frequency. Within these intervals, however, the radiation induces peaks of the dc current that may be quite comparable to the autonomous current in the absence of the radiation. This change of the dc current is due to the radiation-stimulated transitions between the two resonance levels. With the further growth of the external signal, the peak height saturates and its width starts to grow.

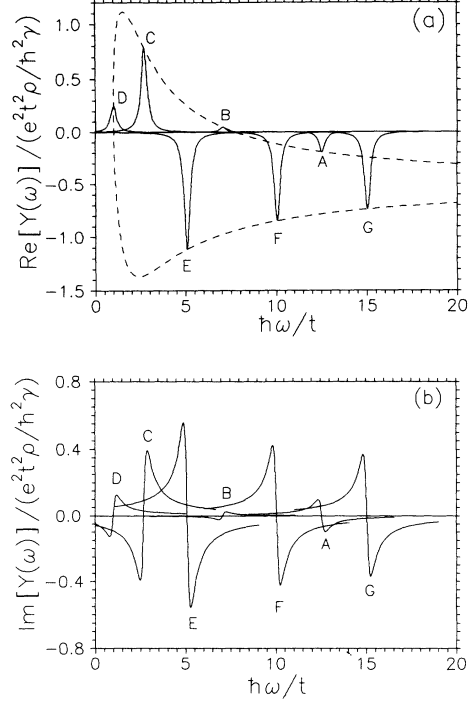


FIG. 4. (a) Real and (b) imaginary parts of the small-signal admittance $Y(\omega)$ due to tunneling between the wells as a function of signal frequency for $\Gamma/\Gamma_e = 3$, $\eta = 1/3$, $\hbar\gamma/t = 0.2$, and several values of the dc voltage [corresponding to the points in Fig. 2(b)]. Dashed line in (a) shows the amplitude of the peak of the real part of the rf admittance (i.e., the rf conductance) as a function of the Bloch oscillation frequency.

allowing $\tilde{\delta}$ to be of the order of Γ , $\Gamma_{L,R}$. In this case one can calculate the new terms in the right-hand sides of Eqs. (13) (arising due to external radiation) in the first approximation in V_A :

$$\pm i\eta \frac{eV_A}{\hbar} \sin\phi \cos\phi \text{Im}R_p,$$

and solve the resulting modified equations together with Eq. (27). The result,

VI. ZERO-POINT OSCILLATIONS AND AVAILABLE POWER

As was mentioned in Sec. IV, the calculated spectral density $S_I(\omega)$ contains a contribution due to the zero-point oscillations in the system. According to the fluctuation-dissipation theorem (applied to a small external ohmic rf load being kept at $T = 0$), this contribution can be calculated as²⁰

$$S_I^{(0)}(\omega) = 4 \frac{\hbar\omega}{2} \text{Re}Y(\omega),$$

where $\text{Re}Y(\omega)$ is the rf conductance found in the previous section.

Now we can find the power density which is radiated into a cold external load represented by its effective impedance $Z_e(\omega)$ (as seen by the double-well structure), under condition that $|Z_e(\omega)| \ll |Y(\omega)|^{-1}$:

$$S_P(\omega) = \eta^2 \text{Re} Z_e(\omega) [S_I(\omega) - S_I^{(0)}(\omega)]. \quad (33)$$

The factor η^2 enters because the rf current in the load is $I_e(t) = \eta I(t)$ rather than $I(t)$ [see Eq. (31) and its discussion].

According to Eqs. (13), (22), (24), (30), and (33) the available power density is

$$S_P(\omega) = \eta^2 \text{Re} Z_e(\omega) \frac{e^2 t^2}{2\hbar^2} \frac{\gamma}{(\omega - \omega_B)^2 + \gamma^2} \times \sum_p 2n_1(p) [1 - n_2(p)]. \quad (34)$$

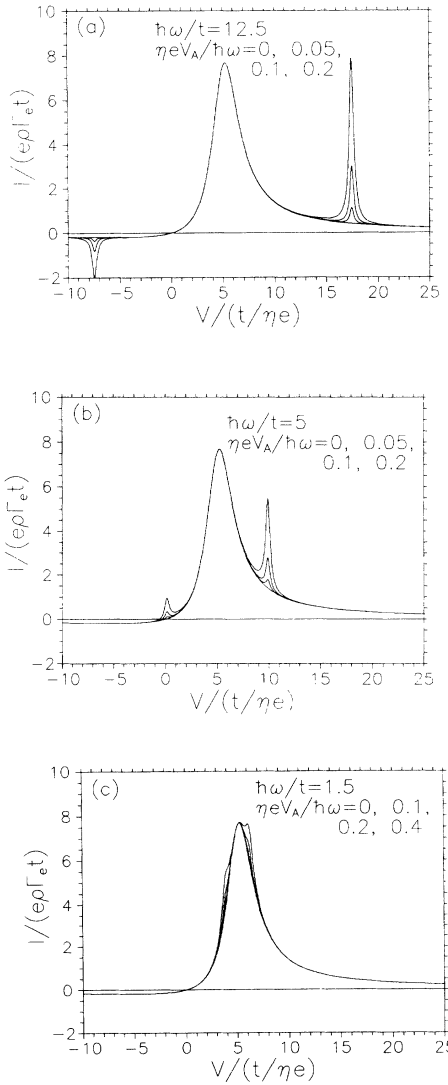


FIG. 5. DC $I - V$ characteristic of an asymmetrical double-well structure (with $\delta_0 = -5t$, $\Gamma/\Gamma_e = 3$, $\hbar\gamma/t = 0.2$, and $\eta = 1/3$), for several values of the amplitude V_A and frequency ω of external radiation: (a) $\hbar\omega/t = 12.5$, (b) $\hbar\omega/t = 5$, (c) $\hbar\omega/t = 1.5$.

In the large-asymmetry limit ($|\delta| \gg t$) and small temperatures the sum in Eq. (34) equals just $2\rho \max\{0, eV \text{sgn}\delta - \Delta\}$. This expression shows clearly that Bloch oscillations can give real power to an external circuit only when the number of electrons in the quantum well with higher quantization level (well 1 in Fig. 1) is larger than that in another well, so that at least a fraction of electrons with higher energy can make a quantum transition to the lower level with radiation of a real (rather than virtual) photon.

Figure 6 shows the net power of the spontaneous Bloch radiation into a small broad-band load $\text{Re} Z_e(\omega) = R_e$,

$$P = \frac{1}{2\pi} \int_{\omega \simeq \omega_B} S_P(\omega) d\omega, \quad (35)$$

as a function of its central frequency ω_B . At large voltages P grows as $(\eta e t/\hbar)^2 \rho |eV - \delta|$. Unfortunately, our present model (valid only for $R_e \ll Y^{-1}$) does not allow calculation of the maximum radiation power P_{\max} , which should be achieved at $R_e \sim Y^{-1}$. A proper generalization of the model, calculation of P_{\max} , and quantitative estimations of the power obtainable from real heterostructures are presently in progress.

VII. DISCUSSION

Statistical characteristics calculated in this work enable us to discuss similarities and differences between the Bloch oscillations and other well-known generators of the narrow-band radiation. Such a discussion is even more relevant in light of some recent publications (e.g., Ref. 23) where the statistical nature of the Bloch oscillations was not taken into account and they were pictured as a direct analog of the Josephson oscillations. This is why we will start our comparison with Josephson oscillations.

A. Josephson oscillations

Frequency ω_J of the Josephson oscillations is exactly related as $\omega_J = \Delta W/\hbar$ to the change of energy of the Cooper pair passing through the Josephson junction (see, e.g., Ref. 24). In this aspect they are really similar to

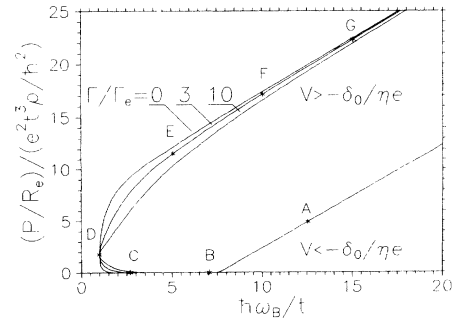


FIG. 6. Net power of the spontaneous Bloch radiation into a small broad-band load R_e as a function of the central frequency ω_B of the radiation, for $\eta = 1/3$ and several values of the Γ/Γ_e ratio. The curves practically coincide in the region $V < -\delta_0/\eta e$, and do not depend on $\hbar\gamma/t$ at $\hbar\gamma \ll t$.

the Bloch oscillations in semiconductor heterostructures. However, the Cooper pairs in the superconducting electrodes of a Josephson junction form a coherent quantum condensate, i.e., their wave functions are completely correlated. Thus, the Josephson oscillations are a sum of *completely correlated* quantum transitions of the Cooper pairs. As a result, the net amplitude of these oscillations is virtually constant even if the phase fluctuations are considerable and the radiation line is relatively broad.²⁴ Hence, despite the fact that the spectral density $S_I(\omega)$ of the Josephson oscillations may look quite similar to that shown in Fig. 3, the statistical density distribution $\rho(A)$ of their amplitude is close to $\delta(A - A_0)$ (the same is true, of course, for any well-developed classical oscillators, lasers well above their excitation threshold, etc.).

In contrast, the Bloch oscillations are a sum of independent contributions of quantum transitions of uncorrelated electrons. This fact results in the broad probability distribution of their amplitude — see Eq. (25). Such a distribution is typical for spontaneous radiation in other quantum systems and for any wide-band noise passed through a narrow-band filter.

B. Tien-Gordon systems

Opposite to the Josephson oscillations is a limit of completely uncorrelated systems, e.g., single-barrier tunnel junctions and other two-terminal structures which obey the Tien-Gordon theory.²⁵ The main result of this theory was that the dc $I - V$ characteristic of the structure in the presence of an external rf voltage with amplitude V_A and frequency ω can always be expressed via its autonomous $I - V$ characteristic (for $V_A = 0$):

$$\bar{I}(V, V_A) = \sum_n J_n^2 \left(\frac{eV_A}{\hbar\omega} \right) \bar{I} \left(V + n \frac{\hbar\omega}{e}, 0 \right), \quad (36)$$

where $J_n(x)$ are the Bessel functions of the first kind. Other results for such Tien-Gordon systems are that the spectral density $S_I(\omega)$ of their current and the small-signal conductance $\text{Re}Y(\omega)$ can also be uniquely expressed via the autonomous dc $I - V$ characteristic:^{26,27}

$$S_I(\omega) = e \sum_{\pm} \bar{I}(V \pm \hbar\omega/e, 0) \coth \left\{ \frac{eV \pm \hbar\omega}{2T} \right\}, \quad (37)$$

$$\text{Re}Y(\omega) = \frac{e}{2\hbar\omega} \left[\bar{I} \left(V + \frac{\hbar\omega}{e}, 0 \right) - \bar{I} \left(V - \frac{\hbar\omega}{e}, 0 \right) \right]. \quad (38)$$

The Tien-Gordon model was first developed to describe quasiparticle (rather than Josephson) tunneling in superconducting junctions,^{25–27} but later Eqs. (36)–(38) were repeatedly derived for systems with quite different mechanisms of electron transfer (see, e.g., Ref. 28). Presently, it is believed that these equations are valid for any two-terminal system which satisfies two conditions.

(1) Electron wave functions on the left and right of the system are incoherent both for the same electron and for different electrons (these conditions are violated and hence Eqs. (37), (38) are not applicable, e.g., in the ballistic channels,³⁰ or Cooper-paired electrons in Josephson junctions²⁴).

(2) Each electron passes the system in a single “leap,” and the leaps of different electrons are uncorrelated (in contrast, e.g., to the situation in systems with correlated single-electron tunneling; see, e.g., Ref. 31).

On the basis of the previous discussion, one might think that the Bloch oscillator considered in this work might satisfy these conditions, and its characteristics should obey Eqs. (36)–(38). Nevertheless, this is not completely true. In fact, according to these equations the videoresponse, spectral density, and rf conductance, considered as functions of $(\hbar\omega/e)$, should closely reproduce all resonance peaks of the autonomous dc $I - V$ curve. By contrast, for our double-well system, the width of the peak in the autonomous dc $I - V$ curve is determined by the interwell tunneling amplitude t , while the peaks in videoresponse, spectral density and rf conductance are determined by the (much smaller) scattering parameter γ .²⁹ (For the videoresponse, this fact was first noticed by Gurvitz.²¹)

There are two reasons for such a difference.

(1) When the levels in the two wells are close ($|\delta| \sim t$), the external dc voltage affects substantially the basic energy spectrum of the system; see Eq. (7).

(2) Even outside this region (i.e., at $|\delta| \gg t$), if scattering and tunneling rates Γ , $\Gamma_{L,R}$ are strongly different, the electron population of the energy levels can be far from thermal equilibrium (i.e., different from that of the corresponding external electrodes).

Both these effects are localized within the range $\Delta\delta$ (18). It is straightforward to check that if all “photon points” $V + n\hbar\omega/e$ in Eqs. (36)–(38) avoid this range, and $\eta = 1$, these equations describe all our results.

To summarize, we have carried out an analysis of the statistical properties of spontaneous Bloch oscillations generated by the double-well semiconductor structures. Our results show, in particular, that this process is closer to noise generated by other simple physical systems with uncorrelated transfer of incoherent electrons than to self-oscillations in the classical meaning of the word. On the other hand, inversion of level population in these structures may allow their use as generators of coherent stimulated radiation in the terahertz frequency band. The statistical properties of such “tasers” would be similar to those of the lasers.

ACKNOWLEDGMENTS

We are grateful to D. K. Ferry for attracting our attention to Ref. 16, and to all participants of the ARO Workshop on Bloch Oscillations (Research Triangle Park, NC, September 1993) for a useful discussion of our results.

- ¹H.M. James, Phys. Rev. **76**, 1611 (1949).
- ²G.H. Wannier, Phys. Rev. **117**, 432 (1960).
- ³L.V. Keldysh, Zh. Eksp. Teor. Fiz. **43**, 661 (1962) [Sov. Phys. JETP **16**, 471 (1963)].
- ⁴L. Esaki and R. Tsu, IBM J. Res. Dev. **14**, 61 (1970).
- ⁵P.A. Lebowitz and R. Tsu, J. Appl. Phys. **41**, 2664 (1970).
- ⁶A. Ya. Shik, Fiz. Tekh. Poluprovodn. **8**, 1841 (1974) [Sov. Phys. Semicond. **8**, 1195 (1975)].
- ⁷F.G. Bass and A.P. Teterevov, Phys. Rep. **140**, 237 (1986).
- ⁸E.E. Mendez and G. Bastard, Phys. Today **46**, 34 (1993).
- ⁹R. Kazarinov and R.A. Suris, Fiz. Tekh. Poluprovodn. **5**, 797 (1971) [Sov. Phys. Semicond. **5**, 707 (1971)]; **6**, 148 (1972) [**6**, 120 (1972)].
- ¹⁰L. Esaki and L.L. Chang, Phys. Rev. Lett. **33**, 495 (1974).
- ¹¹H.T. Grahn, H. Schneider, and K. von Klitzing, Phys. Rev. B **41**, 2890 (1990); H.T. Grahn, R.J. Haug, W. Müller, and K. Ploog, Phys. Rev. Lett. **67**, 1618 (1991).
- ¹²S. Luryi, Solid State Commun. **65**, 787 (1989); IEEE J. Quantum Electron. **27**, 54 (1991).
- ¹³K. Leo, P.H. Bolivar, F. Brüggemann, and R. Schwedler, Solid State Commun. **84**, 943 (1992).
- ¹⁴H.G. Roskos, M.C. Nuss, J. Shah, K. Leo, D.A.B. Miller, A.M. Fox, S. Schmitt-Rink, and K. Köhler, Phys. Rev. Lett. **68**, 2216 (1992).
- ¹⁵C. Waschke, H.G. Roskos, R. Schwedler, K. Leo, H. Kurz, and K. Köhler, Phys. Rev. Lett. **70**, 3319 (1993).
- ¹⁶R.O. Grondin, W. Porod, J. Ho, D.K. Ferry, and G.J. Iafrate, Superlatt. Microstruct. **1**, 183 (1985).
- ¹⁷A simple analysis similar to that for the one-well structure (see, e.g., Ref. 18) shows that the charge-accumulation effects in the double-well structure can lead to an entirely new behavior (bistability) if the effective thickness of the structure d is larger than the Bohr radius a_B . The opposite case ($d \leq a_B$) is within experimental reach, and we will disregard these effects in this work. In an N -layer superlattice ($N \gg 1$), the charge accumulation effects could be disregarded only in the unrealistic case $Nd \leq a_B$.
- ¹⁸D.V. Averin, A. N. Korotkov, and K. K. Likharev, Phys. Rev. B **44**, 6199 (1991).
- ¹⁹W. Kohn and J.M. Luttinger, Phys. Rev. **108**, 590 (1957).
- ²⁰A. Yariv, *Quantum Electronics* (Wiley, New York, 1975), Chap. 8.
- ²¹S.A. Gurvitz, Phys. Rev. B **44**, 11 924 (1991).
- ²²Another important effect is a saturation of the rf admittance $Y(\omega)$, which would be responsible for establishing of stationary oscillations in the "tasers." We will discuss this effect in detail elsewhere.
- ²³A.A. Ignatov, K.F. Renk, and E.P. Dodin, Phys. Rev. Lett. **70**, 1996 (1993).
- ²⁴K.K. Likharev, *Dynamics of Josephson Junctions and Circuits* (Gordon and Breach, New York, 1986), Chaps. 1–4.
- ²⁵P.K. Tien and J.P. Gordon, Phys. Rev. **129**, 647 (1963).
- ²⁶A.J. Dahm, A. Denenstein, D.N. Langenberg, W.H. Parker, D. Rogovin, and D.J. Scalapino, Phys. Rev. Lett. **22**, 1416 (1969).
- ²⁷J.R. Tucker, IEEE J. Quantum Electron. **15**, 1234 (1979).
- ²⁸S.N. Artemenko, A.F. Volkov, and A.V. Zaitsev, Solid State Commun. **30**, 771 (1979).
- ²⁹This statement is not universal, in the opposite limit $\gamma \gg t$ the Tien-Gordon theory is completely applicable to the double-well systems; see, e.g., A.N. Korotkov, D.V. Averin, and K.K. Likharev, Phys. Rev. B **49**, 1915 (1994).
- ³⁰V.A. Khlus, Zh. Eksp. Teor. Fiz. **93**, 2179 (1987) [Sov. Phys. JETP **66**, 1243 (1987)]; G.B. Lesovik, Pis'ma Zh. Eksp. Teor. Fiz. **49**, 513 (1989) [JETP Lett. **49**, 592 (1989)]; M. Buttiker, Phys. Rev. Lett. **65**, 2901 (1990).
- ³¹D.V. Averin and K.K. Likharev, in *Mesoscopic Phenomena in Solids*, edited by B.L. Altshuler, P.A. Lee, and R.A. Webb (Elsevier, Amsterdam, 1991), p. 173.